

Supplementary Information for
Excitable Particles in an Optical Torque Wrench

Francesco Pedaci,* Zhuangxiong Huang,* Maarten van Oene, and Nynke H. Dekker†

*Department of Bionanoscience, Kavli Institute of Nanoscience,
Faculty of Applied Sciences, Delft University of Technology,
Lorentzweg 1, 2628 CJ Delft, The Netherlands*

Stephane Barland

*Institut Non Linéaire de Nice (UMR 6618, UNSA-CNRS),
1361 Route des Lucioles, F-06560 Valbonne, France*

(Dated: October 8, 2010)

*Both authors contributed equally to this work.

†Electronic address: N.H.Dekker@tudelft.nl

Contents**S.I. Deterministic trajectory of a torque spike**

S.I.1. Case: $\omega < \omega_c = \frac{\pi_0}{\gamma}$

S.I.2. Case: $\omega > \omega_c = \frac{\pi_0}{\gamma}$

S.II. Torque spike probability as a function of perturbation amplitude**S.III. Phase locking under periodic perturbations****S.IV. Thermal-noise-driven interspike time distribution****S.V. The average delay time of a torque spike following a perturbation**

S.V.1. The boundaries of the noise-dominated region around the saddle point

S.V.2. The average delay time for perturbation amplitudes $\phi_P > \arccos\left(\frac{\omega}{\omega_c}\right) + L_\theta$

S.V.3. The average delay time for perturbation amplitudes

$$\arccos\left(\frac{\omega}{\omega_c}\right) - L_\theta < \phi_P < \arccos\left(\frac{\omega}{\omega_c}\right) + L_\theta$$

S.V.4. The average delay time for perturbation amplitudes $\phi_P < \arccos\left(\frac{\omega}{\omega_c}\right) - L_\theta$

S.VI. Standard deviation in delay time of torque spike

S.VI.1. Case: the particle jumps into the deterministic region IA

S.VI.2. Case: the particle jumps into the noise-dominated region IIA

S.VI.3. The standard deviation in the delay time for perturbation amplitudes

$$\arccos\left(\frac{\omega}{\omega_c}\right) - L_\theta < \phi_P < \arccos\left(\frac{\omega}{\omega_c}\right) + L_\theta$$

S.VI.4. The standard deviation in the delay time for perturbation amplitudes

$$\phi_P > \arccos\left(\frac{\omega}{\omega_c}\right) + L_\theta$$

S.VII. Measurement of the cylinder's rotational drag through analysis of the torque signal**References**

S.I. DETERMINISTIC TRAJECTORY OF A TORQUE SPIKE

The deterministic behavior of a birefringent particle in OTW can be understood from its noise-free equation of motion (eq.2 in the main text):

$$\dot{x} = -\frac{\tau_0}{\gamma} \sin(2x) - \omega \quad (\text{S.1})$$

S.I.1. Case: $\omega < \omega_c = \frac{\tau_0}{\gamma}$

For $\omega < \omega_c$, eq.S.1 has two stationary solutions (one is stable and the other one is unstable), and one non-stationary solution which describes the trajectory of the system.

Solution 1 (a stable fixed point, or node position):

$$x_n = N\pi - \frac{1}{2} \arcsin\left(\frac{\omega}{\omega_c}\right) \quad (\text{S.2})$$

Solution 2 (an unstable fixed point, or saddle position):

$$x_s = N\pi + \frac{1}{2} \arcsin\left(\frac{\omega}{\omega_c}\right) - \frac{\pi}{2} \quad (\text{S.3})$$

The relaxation from the saddle position to the node position is described by:

$$x = N\pi - \arctan\left(\frac{\omega_c}{\omega} - \sqrt{\left(\frac{\omega_c}{\omega}\right)^2 - 1} + \frac{2\sqrt{\left(\frac{\omega_c}{\omega}\right)^2 - 1}}{1 - C \exp\left(2\sqrt{\omega_c^2 - \omega^2}t\right)}\right) \quad (\text{S.4})$$

where $N \in \mathbb{Z}$, and $C \neq 0$. For $x_n - \pi < x < x_s$, solution 3 can be rewritten as:

$$\cot\left(x + \frac{\pi}{4}\right) = -\sqrt{\frac{\omega_c + \omega}{\omega_c - \omega}} \left[\frac{1 - \exp\left(2\sqrt{\omega_c^2 - \omega^2}(t - t_0)\right)}{1 + \exp\left(2\sqrt{\omega_c^2 - \omega^2}(t - t_0)\right)} \right] \quad (\text{S.5})$$

where t_0 is the time at which $x = (N - \frac{3}{4})\pi$ is reached, and it is rewritten from constant C as:

$$t_0 = \frac{1}{2\sqrt{\omega_c^2 - \omega^2}} \left[\ln\left(\frac{\omega_c}{\omega} + \sqrt{\left(\frac{\omega_c}{\omega}\right)^2 - 1}\right) - \ln C \right] \quad (\text{S.6})$$

When $\omega \lesssim \omega_c$, eq.S.5 can be approximated as:

$$\cot\left(x + \frac{\pi}{4}\right) \approx (\omega_c + \omega)(t - t_0) \quad (\text{S.7})$$

Under this approximation, the deterministic trajectory of a torque spike (Fig.IIIe in the main text) is given by:

$$\frac{\tau}{\tau_0} = -\sin 2x = \frac{\cot^2\left(x + \frac{\pi}{4}\right) - 1}{\cot^2\left(x + \frac{\pi}{4}\right) + 1} \approx \frac{(\omega_c + \omega)^2 (t - t_0)^2 - 1}{(\omega_c + \omega)^2 (t - t_0)^2 + 1} \quad (\text{S.8})$$

S.I.2. Case: $\omega > \omega_c = \frac{\tau_0}{\gamma}$

For $\omega > \omega_c$, there are no stationary solutions to eq.S.1 anymore since they have merged and disappeared through the saddle-node bifurcation. The only solution of the system is periodic and is described by:

$$\cot\left(x + \frac{\pi}{4}\right) = \sqrt{\frac{\omega + \omega_c}{\omega - \omega_c}} \tan\left[\sqrt{\omega^2 - \omega_c^2} (t - t_0)\right] \quad (\text{S.9})$$

where t_0 is the time at which $x = \left(N - \frac{3}{4}\right)\pi$ is reached. The corresponding expression for torque is then given as:

$$\frac{\tau}{\tau_0} = -\sin 2x = \frac{\left(\frac{\omega + \omega_c}{\omega - \omega_c}\right) \tan^2\left[\sqrt{\omega^2 - \omega_c^2} (t - t_0)\right] - 1}{\left(\frac{\omega + \omega_c}{\omega - \omega_c}\right) \tan^2\left[\sqrt{\omega^2 - \omega_c^2} (t - t_0)\right] + 1} \quad (\text{S.10})$$

which indicates the torque signal becomes a periodic function with a period given as:

$$T_{torque} = \frac{\pi}{\sqrt{\omega^2 - \omega_c^2}} \quad (\text{S.11})$$

S.II. TORQUE SPIKE PROBABILITY AS A FUNCTION OF PERTURBATION AMPLITUDE

In the following we consider the behavior of the system under the effect of single external perturbations and we find the expression for the probability to trigger a torque spike as a function of the perturbation amplitude. We note that this statistical approach can explain our experimental data (Fig.III main text) where the perturbation is inserted periodically at very long intervals of time, however a more complete model is needed to explain the more complex behavior which appears in forced excitable systems (S.III) [1].

In the presence of thermal noise, the equation of motion for a birefringent particle (eq.S.1) is rewritten as:

$$\dot{x} + \frac{\tau_0}{\gamma} \sin 2x + \omega + F(t) = 0 \quad (\text{S.12})$$

where $F(t)$ is thermal noise given by:

$$\langle F(t) F(t') \rangle = \frac{2k_B T}{\gamma} \delta(t - t') \quad (\text{S.13})$$

When a birefringent particle in the OTW is subjected to external perturbations (Fig.III main text), its dynamical response is affected by thermal noise in two principal ways:

First, even before the application of a perturbation, the position of the birefringent particle, x_0 , is broadened by thermal noise around the node position. Specifically, the distribution of x_0 is given by Maxwell–Boltzmann statistics as:

$$P_i(x_0) = \frac{1}{\sqrt{\pi \frac{2k_B T}{\kappa}}} \exp\left(-\frac{\frac{1}{2}\kappa(x_0 - x_n)^2}{k_B T}\right) \quad (\text{S.14})$$

where the subscript i at the left-hand side indicates ‘initial position’ (i.e. the particle position prior to the application of perturbation), and κ is the angular trap stiffness at the node position given as:

$$\kappa = -\left.\frac{d\tau}{dx}\right|_{x=x_n} = \left.\frac{d}{dx}\tau_0 \sin(2x)\right|_{x=x_n} = 2\tau_0 \cos(2x_n) = 2\tau_0 \sqrt{1 - \left(\frac{\omega}{\omega_c}\right)^2} \quad (\text{S.15})$$

Second, when a perturbation of sufficient amplitude is applied, the position of the birefringent particle can undergo a sudden jump into the proximity of the saddle position, where the dynamics of the birefringent particle are mainly governed by thermal diffusion (see Sec.S.V, below). In this case, the thermally-driven particle may diffuse further away and trigger a torque spike, or alternatively, may diffuse back towards the node position without triggering a torque spike. The precise spike probability can be derived analytically by expanding the equation of motion around the saddle position as:

$$\dot{\xi} = \lambda \xi + F(t) \quad (\text{S.16})$$

where $\xi = x - x_s$ is a small quantity, and $\lambda = 2\sqrt{\omega_c^2 - \omega^2}$.

Following the approach of ref.[2], we can derive from eq.S.16 the probability that at time t the particle still remains in a semi-infinite box $(-\delta, +\infty)$ (a torque spike will be triggered if the particle diffuse out of this semi-infinite box as described in ref.[2]) given an initial condition $\xi = \xi_0$, as:

$$G_s(\xi_0, t) = \frac{1}{2} [1 + \text{erf}(z(\xi_0, t))] \quad (\text{S.17})$$

where $z(\xi_0, t)$ is given by:

$$z(\xi_0, t) = (\delta + \xi_0 e^{\lambda t}) \left[2 \frac{k_B T}{\gamma \lambda} (e^{2\lambda t} - 1) \right]^{-1/2} \quad (\text{S.18})$$

where $-\delta$ is the leftmost side of the imaginary box defined as in ref.[2].

Putting this all together, the probability that a torque spike is triggered following a perturbation is given by:

$$P(\phi_P) = \int P_i(x_0) [1 - G_s(\xi_0, \tau_p)] dx_0 \quad (\text{S.19})$$

$$\xi_0 = x_0 - x_s - \phi_P$$

where x_0 is the initial position of the particle before perturbation, $P_i(x_0)$ is the distribution of x_0 given by eq.S.14, ϕ_P is the perturbation amplitude, and τ_p is the interval between perturbation events. Since in our experimental configuration, $\lambda\tau_p \gg 1$ the expression for z (eq.S.18) can be simplified to:

$$z(\xi_0, \tau_p) \approx \xi_0 \sqrt{\frac{\gamma \lambda}{2k_B T}} = \sqrt{\frac{\tau_0}{k_B T}} \left[1 - \left(\frac{\omega}{\omega_c} \right)^2 \right]^{1/4} (x_0 - x_s - \phi_P) \quad (\text{S.20})$$

Then computing the integral in eq.S.19, the probability that a torque spike is triggered by a given perturbation amplitude can be written as:

$$P(\phi_P) = \frac{1}{2} \left[1 - \text{erf} \left\{ -\sqrt{\frac{\tau_0}{2k_B T}} \left[1 - \left(\frac{\omega}{\omega_c} \right)^2 \right]^{1/4} \left[\phi_P - \arcsin \left(\frac{\omega}{\omega_c} \right) \right] \right\} \right] \quad (\text{S.21})$$

This is the functional relationship to which the data in Fig.IIIId (main text) is fitted.

S.III. PHASE LOCKING UNDER PERIODIC PERTURBATIONS

Forcing an excitable system with a periodic perturbation, as done in Fig.III (main text), may lead to complex behaviors including phase locking, quasi-periodicity and deterministic chaos [1]. In particular, regions of different locking ratio between perturbations and excited spikes are expected when varying both the perturbation amplitude and period. These regions are indicated by the symbol $n : m$, where n is the number of excited responses in an interval of time which contains m periods of the exciting perturbation. Even richer phenomena may take place in systems that also include stochastic effects [3], such as the micrometer-sized cylinder immersed in fluid under investigation in our experiments.

In the experiments described in Fig.IIIId of the main text, we probe the driven response of our rotating cylinder at fixed forcing frequency but variable amplitude. Here we find that the spike probability as a function of excitation amplitude follows a sigmoidal response that can be fit by an analytical expression based on a statistical escape model (section S.II), justified by the long period chosen for the experimental perturbation.

Here, we briefly explore the combined effects of noise and periodic forcing in our system in Fig.S.I, specifically varying the perturbation period. We plot the probability distribution of the measured inter-spike time under the application of perturbations of decreasing periods when the system is in the excitable regime. The amplitude of the perturbation is kept fixed at a value ($\phi_P = 0.38 \text{ rad}$) at which the probability to excite one spike with a single perturbation is less than 0.5 (compare with Fig.IIIId, main text). For relatively long perturbation periods, we observe the presence of multiple peaks in the histograms. Their precise relative amplitudes may warrant further study taking into account both the external periodic forcing and the presence of thermal noise along the lines of studies such as reference [1]. However, as the forcing period is gradually reduced, one can observe that the probability distribution shifts, until a forcing period of short enough duration is achieved that the response of the system mostly happens close to the 1:2 locking ratio (bottom panel), indicating that deterministic effects strongly dominate the dynamics.

S.IV. THERMAL-NOISE-DRIVEN INTERSPIKE TIME DISTRIBUTION

Eguia *et al.*[2] have shown that the interspike time distribution (in the high friction approximation, which is also the case in our experiments) can be written as a product of a step-like function and a Kramers exponential decay function (eq.5 in the main text):

$$P(t) = AW_{tr}e^{-Kt} \quad (\text{S.22})$$

where the step-like function W_{tr} describes the transient behavior that the particle undergoes following its injection into the imaginary box, as defined in ref.[2], and prior to reaching a stationary distribution. The expression for W_{tr} is given in ref.[2] as:

$$W_{tr}(x_0, t) = \frac{1}{\sqrt{2\pi \left(\frac{R}{\lambda} (1 - e^{-2\lambda t})\right)}} \exp \left[-\frac{(x_h + x_0 e^{-\lambda t})^2}{2\frac{R}{\lambda} (1 - e^{-2\lambda t})} \right] \quad (\text{S.23})$$

where all the parameters are defined in ref.[2]. However, it is difficult to apply this functional form of W_{tr} directly to the data in Fig.IV(main text), because it has too many free parameters. Fortunately, it is possible to derive an alternative expression for W_{tr} suited to our experimental conditions that includes fewer free parameters and facilitates data fitting, as we now demonstrate.

The maximum value of the step-like function is:

$$W_{tr}(x_0, \infty) = \frac{1}{\sqrt{2\pi\frac{R}{\lambda}}} \exp\left(-\frac{x_h^2}{2\frac{R}{\lambda}}\right) \quad (\text{S.24})$$

allowing us to rescale W_{tr} as:

$$\begin{aligned} \tilde{W}_{tr}(t) &= \frac{W_{tr}(x_0, t)}{W_{tr}(x_0, \infty)} \\ &= \frac{1}{\sqrt{1 - e^{-2\lambda t}}} \exp\left\{ \frac{x_h^2}{2\frac{R}{\lambda}} \left(\left[\left(\frac{x_0}{x_h}\right)^2 + 1 \right] - \frac{\left[\left(\frac{x_0}{x_h}\right)^2 + 1 \right] - 2\frac{x_0}{x_h}e^{-\lambda t}}{1 - e^{-2\lambda t}} \right) \right\} \end{aligned} \quad (\text{S.25})$$

Since $|x_h| \ll |x_0|$, especially when the excitable system is close to the critical point (as in our experiments), we have:

$$\tilde{W}_{tr}(t) \approx \frac{1}{\sqrt{1 - e^{-2\lambda t}}} \exp\left[-\left(\frac{\lambda x_0^2}{2R}\right) \frac{1}{e^{2\lambda t} - 1}\right] \quad (\text{S.26})$$

which can be further simplified using the midpoint of the step-like function (i.e. half height of the step-like function at $t = s$):

$$\tilde{W}_{tr}(s) = \frac{1}{2}. \quad (\text{S.27})$$

Then we have:

$$\frac{\lambda x_0^2}{2R} = (e^{2\lambda s} - 1) \ln \frac{2e^{\lambda s}}{\sqrt{e^{2\lambda s} - 1}} \approx (e^{2\lambda s} - 1) \ln 2 \quad (\text{S.28})$$

Putting this all together, we have:

$$\tilde{W}_{tr}(t) \approx \frac{1}{\sqrt{1 - e^{-2\lambda t}}} \exp\left[-\frac{e^{2\lambda s} - 1}{e^{2\lambda t} - 1} \ln 2\right] \quad (\text{S.29})$$

Now there are only two free parameters in the expression for the step-like function.

In the spirit of ref.[2], when the evolution time interval (also called the refractory time t_0) from the saddle point to the next injection point is taken into account, the step-like function

can be rewritten approximately as:

$$\begin{cases} \tilde{W}_{tr}(t) \approx \frac{1}{\sqrt{1-e^{-2\lambda(t-t_0)}}} \exp\left[-\frac{e^{2\lambda(s-t_0)}-1}{e^{2\lambda(t-t_0)}-1} \ln 2\right] & \text{if } t \geq t_0 \\ \tilde{W}_{tr}(t) = 0 & \text{if } t < t_0 \end{cases} \quad (\text{S.30})$$

which is the expression of step-like function employed in the data fitting in Fig.IV(main text).

S.V. THE AVERAGE DELAY TIME OF A TORQUE SPIKE FOLLOWING A PERTURBATION

As shown in Fig.S.II, when subjected to a perturbation of a certain amplitude, the birefringent particle will suddenly jump from its original position around the node point (region IIB in Fig.S.II) into the proximity of the saddle position where the dynamics are dominated by thermal noise (region IIA in Fig.S.II). However, if the perturbation amplitude is either too small or too large, the particle may jump into other regions where the thermal noise is not a dominant dynamical factor (region IA and IB in Fig.S.II). Below we will derive the expressions for the average delay time between the application of the perturbation and the detection of a torque spike, for different ranges of perturbation amplitudes. The application of the analytical expressions to our experimental data is also shown in Fig.S.III.

S.V.1. The boundaries of the noise-dominated region around the saddle point

Using a rough approximation, we can define the boundaries of the noise-dominated region around the saddle point at the positions of:

$$|\xi| = \delta = L_\theta \quad (\text{S.31})$$

where $L_\theta = \sqrt{\frac{2k_B T}{\kappa}}$ is called the thermal length. Beyond these boundaries, e.g. $\xi < -\delta$ (region IA in Fig.S.II), the particle is unlikely to roll back by thermal force because the energy barrier that the particle needs to overcome is larger than thermal energy $k_B T$. So in region IA(Fig.S.II), the particle will evolve deterministically away from the saddle point and trigger a torque spike.

S.V.2. The average delay time for perturbation amplitudes $\phi_P > \arccos\left(\frac{\omega}{\omega_c}\right) + L_\theta$

If the particle jumps directly into region IA (Fig.S.II) when subjected to the perturbation, the delay time of the deterministic torque spike ($t_{d,d}$, the first subscript d indicates ‘delay time’, and the second subscript d indicates ‘deterministic’) can be derived from eq.S.7 as:

$$t_{d,d} = \frac{1}{\omega_c + \omega} \left[\cot \left(\xi_{th} + \frac{1}{2} \arcsin \left(\frac{\omega}{\omega_c} \right) - \frac{\pi}{4} \right) - \cot \left(\xi_0 + \frac{1}{2} \arcsin \left(\frac{\omega}{\omega_c} \right) - \frac{\pi}{4} \right) \right] \quad (\text{S.32})$$

where $\xi_0 = x_0 - x_s - \phi_P$ is the initial position of the particle right after perturbation and ξ_{th} is the threshold position (the subscripts th are short for ‘threshold’) where a torque spike can be detected. To analyze our experiments, we set $\xi_{th} = -\frac{1}{2} \arcsin\left(\frac{\omega}{\omega_c}\right)$ for the convenience of data processing and analysis. Then we have:

$$t_{d,d} = \frac{1}{\omega_c + \omega} \left[\cot \left(\frac{\pi}{4} - \frac{1}{2} \arcsin \left(\frac{\omega}{\omega_c} \right) - \xi_0 \right) - 1 \right] \quad (\text{S.33})$$

From the previous section (Sec.S.II), we know that for a given perturbation amplitude ϕ_P , ξ_0 is not a fixed value; instead, due to thermal broadening of x_0 around the node position, ξ_0 has a distribution given by eq.S.14 as:

$$P_\theta(\xi_0) = \frac{1}{\sqrt{\pi L_\theta^2}} \exp \left[-\frac{(\xi_0 - \bar{\xi}_0)^2}{L_\theta^2} \right] \quad (\text{S.34})$$

$$\bar{\xi}_0 = \arccos \left(\frac{\omega}{\omega_c} \right) - \phi_P$$

When subjected to a perturbation of $\phi_P > \arccos\left(\frac{\omega}{\omega_c}\right) + L_\theta$ (i.e. $\bar{\xi}_0 < -\delta$, region IA in Fig.S.II), the birefringent particle is much less likely to jump into the noise-dominated region IIA (Fig.S.II). In this case, the average delay time $\langle t_d \rangle_{P,b}$ (the first subscript d indicates ‘delay time’, the second subscript P indicates an average for a given ‘perturbation amplitude’, and the last subscript b indicates that the perturbation amplitude is ‘big’ $\phi_P > \arccos\left(\frac{\omega}{\omega_c}\right) + L_\theta$.) between the application of the perturbation and the detection of a torque spike (when the particle evolves to ξ_{th}) is approximately given by:

$$\langle t_d \rangle_{P,b} \approx \int t_{d,d}(\xi_0) P_\theta(\xi_0) d\xi_0$$

$$\langle t_d \rangle_{P,b} \approx \frac{\int_{\bar{\xi}_0 - L_\theta}^{\bar{\xi}_0 + L_\theta} t_d(\xi_0) d\xi_0}{\int_{\bar{\xi}_0 - L_\theta}^{\bar{\xi}_0 + L_\theta} d\xi_0} \approx \frac{1}{\omega_c + \omega} \left[\cot \left(\phi_P - \frac{1}{2} \arccos \left(\frac{\omega}{\omega_c} \right) - L_\theta \right) - 1 \right] \quad (\text{S.35})$$

This expression is used to fit to the experimental data in Fig.S.III (black curves at right).

S.V.3. The average delay time for perturbation amplitudes $\arccos\left(\frac{\omega}{\omega_c}\right) - L_\theta < \phi_P < \arccos\left(\frac{\omega}{\omega_c}\right) + L_\theta$

If the particle jumps into the noise-dominated region IIA ($-\delta < \xi_0 < \delta$, Fig.S.II) following the perturbation, it may evolve into a torque spike, or alternatively diffuse back into the node position. Events which successfully evolve into torque spikes must first diffuse into the deterministic region IA (Fig.S.II) and then take the deterministic path to ξ_{th} . Thus the delay time ($t_{d,n}$, the first subscript d indicates ‘delay time’, and the second subscript n indicates ‘noise-dominated’) between the application of the perturbation and the detection of a torque spike is given as:

$$t_{d,n} = t_\delta + t_{\delta-th}. \quad (\text{S.36})$$

Here $t_{\delta-th}$ which represents the deterministic evolution time from the boundary of region IA ($\xi_0 = -\delta$, Fig.S.II) to the threshold position where a torque spike can be detected (ξ_{th} , Fig.S.II), can be calculated using eq.S.33 as:

$$t_{\delta-th} = \frac{1}{\omega_c + \omega} \left[\cot\left(\frac{\pi}{4} - \frac{1}{2} \arcsin\left(\frac{\omega}{\omega_c}\right) + \delta\right) - 1 \right] \quad (\text{S.37})$$

t_δ is the stochastic escape time that the particle evolve out of the noise-dominated region IIA(Fig.S.II), which has a distribution that can be derived from eq.S.17 as:

$$P_d(\xi_0, t_\delta) = -\frac{d}{dt} G_s(\xi_0, t) = W_{tr}(\xi_0, t_\delta) \frac{(\xi_0 + \delta e^{\lambda t_\delta}) \lambda}{(e^{2\lambda t_\delta} - 1)} \quad (\text{S.38})$$

where $W_{tr}(\xi_0, t_\delta)$ is a step-like function given as:

$$W_{tr}(\xi_0, t_\delta) = \frac{1}{\sqrt{\pi L_\theta^2 (1 - e^{-2\lambda t_\delta})}} \exp\left[-\frac{1}{L_\theta^2} \frac{(\delta e^{-\lambda t_\delta} + \xi_0)^2}{(1 - e^{-2\lambda t_\delta})}\right] \quad (\text{S.39})$$

The midpoint (t_m) of this step-like function can be derived approximately as:

$$t_m \approx \frac{1}{2\lambda} \ln\left(\frac{\delta^2}{(\ln 2) L_\theta^2} + 1\right) = \frac{1}{2\lambda} \ln\left(\frac{1}{\ln 2} + 1\right) \quad (\text{S.40})$$

In the spirit of ref.[2], if we further approximate the step-like function by a Heaviside function, then the average escape time $\langle t_\delta \rangle$ for a particle that jumps into noise-dominated region

following a perturbation.) can be calculated as:

$$\begin{aligned} \langle t_\delta \rangle &= \frac{\int t_\delta P_d(\xi_0, t_\delta) dt}{\int P_d(\xi_0, t_\delta) dt} \\ &\approx \frac{W_{tr}(\xi_0, \infty) \int_{t_m}^\infty t_\delta \frac{(\xi_0 + \delta e^{\lambda t_\delta})^\lambda}{(e^{2\lambda t_\delta} - 1)} dt}{W_{tr}(\xi_0, \infty) \int_{t_m}^\infty \frac{(\xi_0 + \delta e^{\lambda t_\delta})^\lambda}{(e^{2\lambda t_\delta} - 1)} dt} \approx \frac{\int_{t_m}^\infty t_\delta \frac{e^{\lambda t_\delta}}{e^{2\lambda t_\delta} - 1} dt}{\int_{t_m}^\infty \frac{e^{\lambda t_\delta}}{e^{2\lambda t_\delta} - 1} dt} \approx t_m + \frac{1}{\lambda} \end{aligned} \quad (\text{S.41})$$

Therefore for a particle that jumps into the noise-dominated region IIA ($-\delta < \xi_0 < \delta$, Fig.S.II) following the perturbation, the average delay time $\langle t_{d,n} \rangle$ between the application of the perturbation and the detection of a torque spike is given as:

$$\begin{aligned} \langle t_{d,n} \rangle &= \langle t_\delta \rangle + t_{\delta-th} \\ &= \frac{1}{2\lambda} \ln \left(\frac{1}{\ln 2} + 1 \right) + \frac{1}{\lambda} + \frac{1}{\omega_c + \omega} \left[\cot \left(\frac{\pi}{4} - \frac{1}{2} \arcsin \left(\frac{\omega}{\omega_c} \right) + L_\theta \right) - 1 \right] \end{aligned} \quad (\text{S.42})$$

As discussed above, due to the thermal broadening of x_0 around the node position (Sec.S.II), for a given perturbation amplitude ϕ_P (and thus given $\bar{\xi}_0$), not all particles can jump into region IIA ($-\delta < \xi_0 < \delta$, Fig.S.II). So events that the particle jumps into region IA ($\xi_0 < -\delta$, Fig.S.II) should also be taken into account. Using a rough approximation, we can assume all the particles (given $-\delta < \bar{\xi}_0 < \delta$) that jumps into the deterministic region IA ($\xi_0 < -\delta$, Fig.S.II) have the same characteristic delay time given by $t_{\delta-th}$. Then for the perturbation amplitude range of $\arccos \left(\frac{\omega}{\omega_c} \right) - L_\theta < \phi_P < \arccos \left(\frac{\omega}{\omega_c} \right) + L_\theta$, the average delay time $\langle t_d \rangle_{P,m}$ (the first subscript d indicates ‘delay time’, the second subscript P indicates an average for a given ‘perturbation amplitude’, and the last subscript m indicates that the perturbation amplitude is in the ‘medium range’) between the application of the perturbation and the detection of a torque spike is given as:

$$\langle t_d \rangle_{P,m} = \langle t_{d,n} \rangle - \langle t_\delta \rangle (r(\phi_P)) \quad (\text{S.43})$$

where $r(\phi_P)$ is the probability that the particle jumps into the region IA ($\xi_0 < -\delta$, Fig.S.II) following a perturbation given as:

$$\begin{aligned}
r(\phi_P) &= \int_{-\infty}^{-\delta} P_\theta(\xi_0) d\xi_0 \\
&= \frac{1}{2} \left\{ \operatorname{erf} \left[\frac{-\delta - \bar{\xi}_0}{L_\theta} \right] + 1 \right\} \\
&= \frac{1}{2} \left\{ \operatorname{erf} \left[\frac{\phi_P - \arccos\left(\frac{\omega}{\omega_c}\right) - L_\theta}{L_\theta} \right] + 1 \right\} \quad (\text{S.44})
\end{aligned}$$

This expression for $\langle t_d \rangle_{P,m}$ (eq.S.43) is used to fit to the experimental data in Fig.S.III (black curves at left).

S.V.4. The average delay time for perturbation amplitudes $\phi_P < \arccos\left(\frac{\omega}{\omega_c}\right) - L_\theta$

If the perturbation amplitude is too small ($\phi_P < \arccos\left(\frac{\omega}{\omega_c}\right) - L_\theta$), the particle is much more likely to either jump into the deterministic region IB ($\xi_0 > \delta$, Fig.S.II), where the particle will evolve deterministically back to the node position without triggering a torque spike, or alternatively, not even jump out of region IIB (Fig.S.II), where the particle is originally located. Since the analysis of the delay time of torque spike is only valid for the events that trigger a torque spike, the discussion on this range of perturbation amplitude is not relevant.

S.VI. STANDARD DEVIATION IN DELAY TIME OF TORQUE SPIKE

Using the results in the previous section (Sec.S.V), we can also derive the standard deviation in the delay time of torque spike separately for different ranges of perturbation amplitudes.

S.VI.1. Case: the particle jumps into the deterministic region IA

If the particle jumps into the deterministic region IA ($\xi_0 < -\delta$, Fig.S.II) following a perturbation, the standard deviation in the delay time of torque spike can be derived as:

$$\begin{aligned}
\sqrt{\langle (\delta t_{d,d})^2 \rangle} &= \sqrt{\langle t_{d,d}^2 \rangle - \langle t_{d,d} \rangle^2} \\
&\approx \frac{1}{\sqrt{2}} [t_{d,d}(\bar{\xi}_0)] L_\theta = \frac{L_\theta}{\sqrt{2}(\omega_c + \omega)} \sin^{-2} \left(\phi_P - \frac{1}{2} \arccos \left(\frac{\omega}{\omega_c} \right) \right) \quad (\text{S.45})
\end{aligned}$$

where $\langle t_{d,d} \rangle$ and $\langle t_{d,d}^2 \rangle$ are approximately given as:

$$\langle t_{d,d} \rangle = \int t_{d,d}(\xi_0) P_\theta(\xi_0) d\xi_0 \approx t_{d,d}(\bar{\xi}_0) + \frac{1}{4} L_\theta^2 \ddot{t}_{d,d}(\bar{\xi}_0) \approx \langle t_d \rangle_{P,b} \quad (\text{S.46})$$

$$\langle t_{d,d}^2 \rangle = \int t_{d,d}^2(\xi_0) P_\theta(\xi_0) d\xi_0 \approx t_{d,d}^2(\bar{\xi}_0) + \frac{1}{2} \left\{ t_{d,d}(\bar{\xi}_0) \ddot{t}_{d,d}(\bar{\xi}_0) + [t_{d,d}(\bar{\xi}_0)]^2 \right\} L_\theta^2 \quad (\text{S.47})$$

S.VI.2. Case: the particle jumps into the noise-dominated region IIA

If the particle jumps into the noise-dominated region IIA ($|\xi_0| < \delta$, Fig.S.II) following a perturbation, the standard deviation in the delay time of torque spike is given as:

$$\sqrt{\langle (\delta t_{d,n})^2 \rangle} = \sqrt{\langle (\delta t_\delta)^2 \rangle + \langle (\delta t_{\delta-th})^2 \rangle} \quad (\text{S.48})$$

where $\langle (\delta t_{\delta-th})^2 \rangle$ can be calculated directly from eq.S.45 as:

$$\langle (\delta t_{\delta-th})^2 \rangle \approx \frac{L_\theta}{\sqrt{2}(\omega_c + \omega)} \sin^{-2} \left(\frac{1}{2} \arccos \left(\frac{\omega}{\omega_c} \right) + L_\theta \right) \quad (\text{S.49})$$

and $\langle (\delta t_\delta)^2 \rangle$ can be derived approximately as:

$$\langle (\delta t_\delta)^2 \rangle = \langle t_\delta^2 \rangle - \langle t_\delta \rangle^2 \approx \frac{\int_{t_m}^\infty t^2 \frac{e^{\lambda t}}{e^{2\lambda t} - 1} dt}{\int_{t_m}^\infty \frac{e^{\lambda t}}{e^{2\lambda t} - 1} dt} - \left(\frac{\int_{t_m}^\infty t \frac{e^{\lambda t}}{e^{2\lambda t} - 1} dt}{\int_{t_m}^\infty \frac{e^{\lambda t}}{e^{2\lambda t} - 1} dt} \right)^2 = \frac{1}{\lambda^2} \quad (\text{S.50})$$

S.VI.3. The standard deviation in the delay time for perturbation amplitudes

$$\arccos \left(\frac{\omega}{\omega_c} \right) - L_\theta < \phi_P < \arccos \left(\frac{\omega}{\omega_c} \right) + L_\theta$$

As discussed in previous section (Sec.S.V), in the range of perturbation amplitudes $\arccos \left(\frac{\omega}{\omega_c} \right) - L_\theta < \phi_P < \arccos \left(\frac{\omega}{\omega_c} \right) + L_\theta$ (i.e. $-\delta < \bar{\xi}_0 < \delta$), the particle still has a certain probability to jump into the deterministic region IA ($\xi_0 < -\delta$, Fig.S.II). This probability is given by $r(\phi_P)$ (eq.S.44). Again, using a rough approximation, we can assume all the events (given $-\delta < \bar{\xi}_0 < \delta$) that the particle jumps into region IA ($\xi_0 < -\delta$, Fig.S.II) have the same standard deviation in delay time given by $\langle (\delta t_{\delta-th})^2 \rangle$, then the standard deviation in the total delay time $\sqrt{\langle (\delta t_d)^2 \rangle_{P,m}}$ (the first subscript d indicates ‘delay time’, the second subscript P indicates that the standard deviation is calculated for a given ‘perturbation amplitude’, and the last subscript m indicates that the perturbation amplitude is ‘medium’: $\arccos \left(\frac{\omega}{\omega_c} \right) - L_\theta < \phi_P < \arccos \left(\frac{\omega}{\omega_c} \right) + L_\theta$) is found as:

$$\sqrt{\langle (\delta t_d)^2 \rangle_{P,m}} \approx \sqrt{[1 - r(\phi_P)] \langle (\delta t_\delta)^2 \rangle + \langle (\delta t_{\delta-th})^2 \rangle + r(\phi_P) [1 - r(\phi_P)] \langle t_\delta \rangle^2} \quad (\text{S.51})$$

This expression is used to fit to the experimental data in Fig.S.III (red dashed envelope curves at left).

S.VI.4. The standard deviation in the delay time for perturbation amplitudes

$$\phi_P > \arccos\left(\frac{\omega}{\omega_c}\right) + L_\theta$$

Similarly, for a given perturbation amplitude ϕ_P that satisfies $\bar{\xi}_0 < -\delta$ (region IA in Fig.S.II), the chance that the particle jumps into noise-dominated region IIA (Fig.S.II) should also be taken into account. Then the standard deviation in the total delay time $\sqrt{\langle(\delta t_d)^2\rangle_{P,b}}$ (the first subscript d indicates ‘delay time’, the second subscript P indicates that the standard deviation is calculated for a given ‘perturbation amplitude’, and the last subscript b indicates that the perturbation amplitude is ‘big’: $\phi_P > \arccos\left(\frac{\omega}{\omega_c}\right) + L_\theta$) can be calculated as:

$$\sqrt{\langle(\delta t_d)^2\rangle_{P,b}} \approx \sqrt{(1-r(\phi_P))\langle(\delta t_{d,n})^2\rangle + r(\phi_P)\langle(\delta t_{d,d})^2\rangle + r(\phi_P)(1-r(\phi_P))(\langle t_{d,d}\rangle - \langle t_{d,n}\rangle)^2} \quad (\text{S.52})$$

This expression is used to fit to the experimental data in Fig.S.III (red dashed envelope curves at right).

S.VII. MEASUREMENT OF THE CYLINDER’S ROTATIONAL DRAG THROUGH ANALYSIS OF THE TORQUE SIGNAL

The torque signal of a quartz cylinder in OTW encodes information on the rotational drag (γ) experienced by the cylinder. This allows us to extract γ through analysis of the torque signal, both when $\omega > \omega_c$, and when $\omega < \omega_c$, as demonstrated in Fig.Vd in the main text.

When $\omega > \omega_c$, the torque signal appears as (quasi-) periodic spikes. The period of the torque spikes is given in eq.S.11, from which we can determine ω_c . Since the maximum torque τ_0 that can be applied can be read off directly from the torque spike as half of the peak-to-peak amplitude, it follows that we can calculate γ using:

$$\gamma = \frac{\tau_0}{\omega_c} = \tau_0 \left(\omega^2 - \frac{\pi^2}{T_{\text{torque}}^2} \right)^{-\frac{1}{2}} \quad \text{for } \omega > \omega_c \quad (\text{S.53})$$

When $\omega < \omega_c$, no spikes appear in the torque signal (except when ω is very close to ω_c , in which case thermal noise can induce torque spikes as shown in Fig.IV in the main text.).

In this case, γ can be determined via one of two alternative approaches. One approach is to use the equation: $\gamma = \frac{\tau}{\omega}$, where τ is the measured torque signal. Alternatively, one can employ the relationship $\gamma = \frac{\tau_0}{\omega_c}$, where τ_0 is the maximum torque that can be applied, and ω_c is determined from the variance in (non-spike) torque signal $\langle \delta\tau^2 \rangle$ as follows:

First $\langle \delta\tau^2 \rangle$ can be rewritten as:

$$\langle \delta\tau^2 \rangle = \kappa^2 \langle \delta x^2 \rangle \tag{S.54}$$

where $\kappa = 2\tau_0 \sqrt{1 - \left(\frac{\omega}{\omega_c}\right)^2}$ is the angular trapping stiffness at the node position (x_n), and $\langle \delta x^2 \rangle$ is the variance in angular displacement around x_n , which can be calculated by partition function theory from eq.S.14 as:

$$\langle \delta x^2 \rangle = \frac{k_B T}{\kappa} \tag{S.55}$$

Putting this together, we have an expression for ω_c :

$$\frac{\langle \delta\tau^2 \rangle}{2\tau_0 k_B T} = \sqrt{1 - \left(\frac{\omega}{\omega_c}\right)^2} \tag{S.56}$$

and the expression for γ :

$$\gamma = \frac{\tau_0}{\omega_c} = \frac{1}{\omega} \sqrt{\tau_0^2 - \left(\frac{\langle \delta\tau^2 \rangle}{2k_B T}\right)^2} \quad \text{for } \omega < \omega_c \tag{S.57}$$

- [1] Feingold, M., Gonzalez, D. L., Piro, O., Viturro, H. Phys. Rev. A 37(10), 4060–4063 (1988).
- [2] Eguia, M. C. and Mindlin, G. B. Phys. Rev. E 61(6), 6490–6499 (2000).
- [3] Longtin, A. and Chialvo, D. R. Phys. Rev. Lett. 81(18) 4012–4015 (1998).

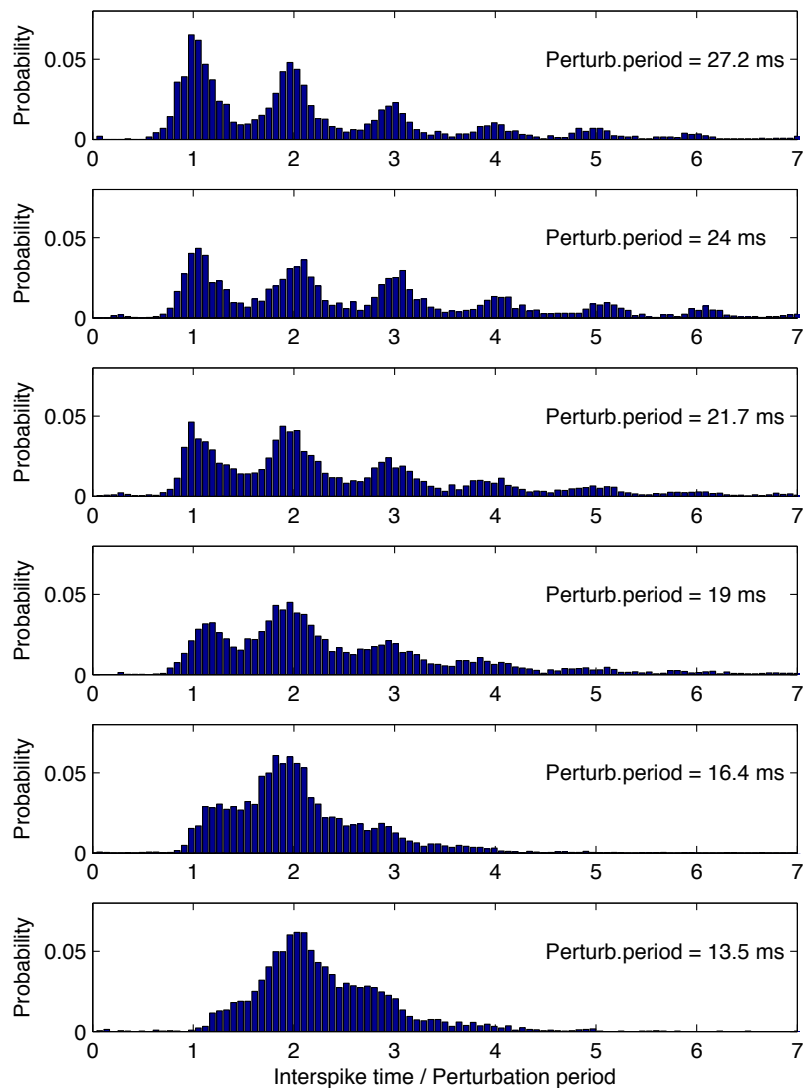


FIG. S.I: **Probability distribution for the interspike-time of events triggered by a periodic external perturbation.** The period of the perturbation is indicated in each panel. Different locking ratios, indicated by the peaks at integer multiples of the perturbation period, are visited by the system forced by long perturbation periods. Decreasing the period of the perturbation changes the relative probability, leaving the 2:1 ratio as the most probable at short period. The amplitude of the perturbation is kept fixed at a value ($\phi_P = 0.38 \text{ rad}$) at which the probability to excite one spike with a single perturbation is less than 0.5.

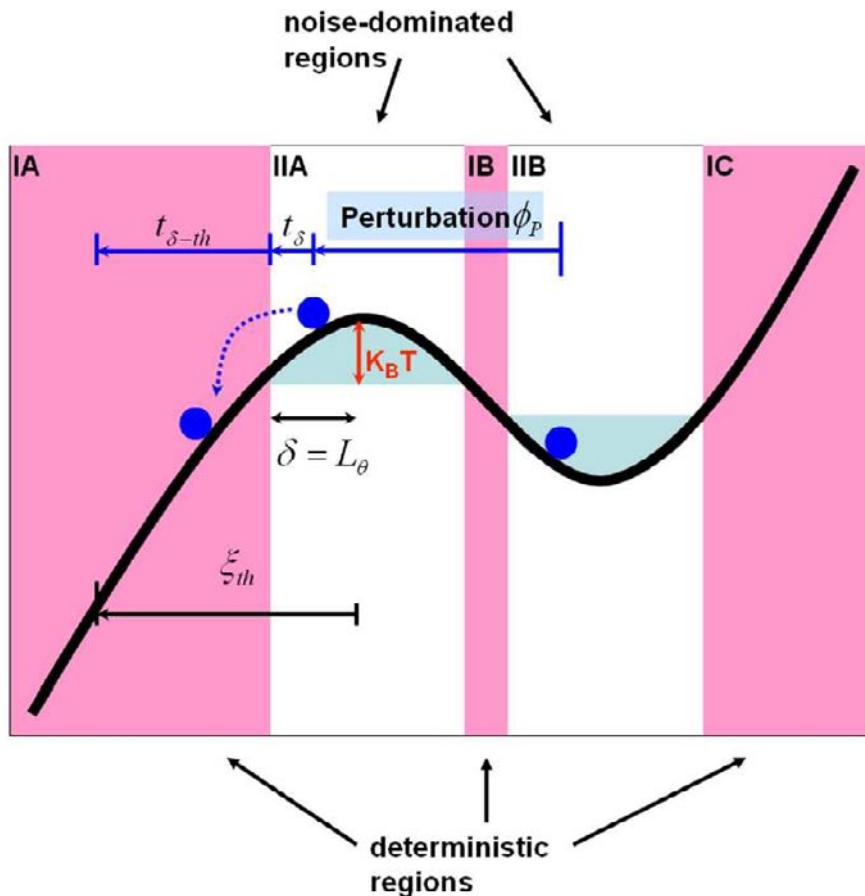


FIG. S.II:

Evolution of a birefringent particle subject to a perturbation. The thick black sinuous curve represents the potential experienced by a birefringent particle (blue circle). The potential profile can be divided into two types of regions. In regions of Type I (deterministic regions, in pink), the behavior of the particle is basically determined by the potential profile only, while in regions of Type II (noise-dominated regions, in white), the behavior of the particle is dominated by the thermal noise. The boundaries between Type I and Type II regions are approximated by going out by one thermal length L_θ beyond the stable or unstable fixed points. When the system is subjected to a perturbation, the particle may jump from its original position in region IIB to other regions, depending on the amplitude of the perturbation. If the particle jumps into region IIA, it may diffuse (indicated by t_δ) across the boundary ($-\delta$) between region IIA and region IA and evolve into a torque spike, or alternatively the particle may diffuse back towards its original position without triggering any torque spike. The threshold position where a triggered torque spike can be detected is indicated by ξ_{th} . The evolution time from the boundary (δ) between region IIA and IA to the threshold position (ξ_{th}) is indicated by $t_{\delta-th}$.

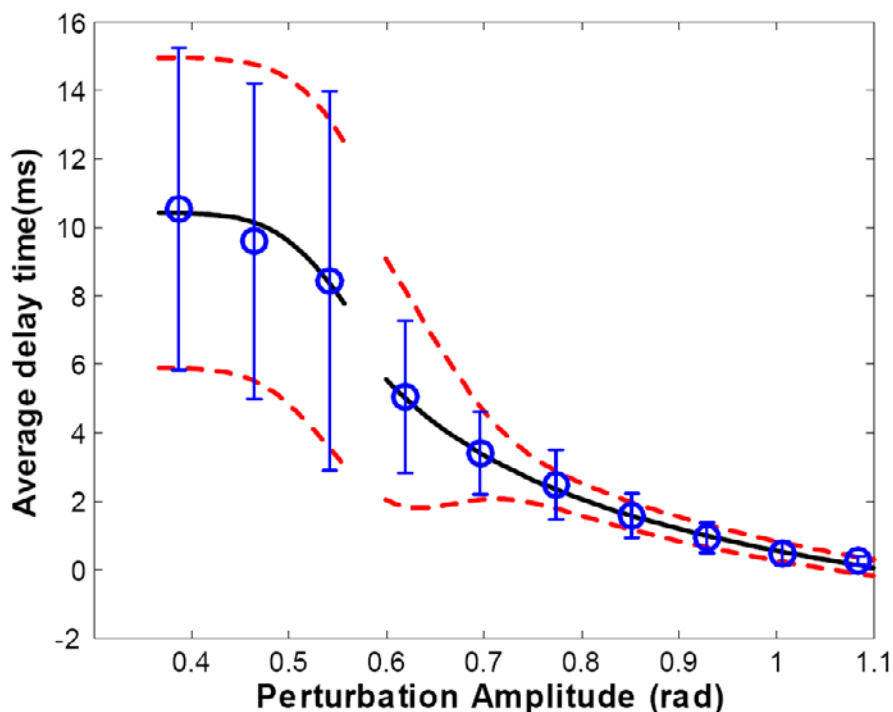


FIG. S.III: Average delay time of a torque spike as a function of perturbation amplitude (ϕ_P). The experimental data is shown in blue circles. The error bars (blue) represent one standard deviation in the delay time, as determined from experimental data. The black line is the fit to eq.S.43 (curve at left) and eq.S.35 (curve at right) using $\lambda = 230$ Hz, $\omega/\omega_c = 0.8862$ and $\tau_0 = 1150$ pN \cdot nm. The envelope (upper and lower red dashed lines) represents the theoretical values of one standard deviation from the mean, calculated using eq.S.51 (curves at left) and eq.S.52 (curves at right) using the same parameters as the black line.